JOURNAL OF Materials CHEMISTRY

Self-assembled organic–inorganic composite superlattice thin films incorporating photo- and electro-chemically active phosphomolybdate anion

Tie Rui Zhang,[a] Wei Feng,[a] Ya Qin Fu,[a] Ran Lu,*[a] Chun Yan Bao,[a] Xin Tong Zhang,[a] Bing Zhao,[b] Chang Qing Sun,[a] Tie Jin Li,[a] Ying Ying Zhao[a] and Jian Nian Yao[c]

[a]*Department of Chemistry, Jilin University, Changchun 130023, P. R. China. E-mail: luran@mail.jlu.edu.cn; Fax: +86-431-8949334*
[b]*Key Laboratory of Supramolecular Structure and Spectroscopy, Jilin University, Changchun 130023, P. R. China*
[c]*Institute of Chemistry and Center for Molecular Science, Chinese Academy of Sciences, Beijing 100080, P. R. China*

Received 29th October 2001, Accepted 20th February 2002
First published as an Advance Article on the web 8th March 2002

A highly ordered multilayer film was formed by casting chloroform solutions of an ionic complex between a dimethyldioctadecylammonium (DODA) and a phosphomolybdate anion $PMo_{12}O_{40}^{3-}$ (PMo_{12}) on a glassy carbon electrode and solid substrates (CaF_2, quartz, and borosilicate glass). A well-ordered lamellar superlattice structure was identified by X-ray diffraction (XRD) and differential scanning calorimetry (DSC) experiments. IR spectra showed that the Keggin structure of the phosphomolybdate anion is preserved in the composite film. The superlattice film showed good photochromic and electrochemical properties. Irradiated with UV light, the transparent film changed from colorless to blue. Then, bleaching occurred when the film was in contact with ambient air or O_2 in the dark. A possible photochromic mechanism was proposed according to electron paramagnetic resonance (EPR), Fourier transform infrared spectra (FTIR), UV–vis spectra, and related literature. The electrochemical behavior of the composite film was also examined by cyclic voltammetry in detail.

Introduction

Polyoxometalates (POM) with well-defined primary structures have recently attracted much attention as building units of novel inorganic materials that have found applications in fields as diverse as catalysis,[1] medicine,[2] biochemistry,[3] material science,[4] and so on. Their structures can be depicted as molecular fragments of close-packed metal oxides with the general formula $X_xM_mO_y^{n-}$ (where M represents Mo, W, V, *etc.* and X represents P, Si, As, *etc.*).[5] The first and best-known type of POM is the so-called Keggin structure, which consists of four M_3O_{13} groups of three edge-shared MO_6 octahedra, each group linked to the next M_3O_{13} by corner sharing and the whole arrangement enclosing a corner-sharing central XO_4 tetrahedron. One of the most important properties of these metal oxide clusters is the capability for reversible multivalence reduction, forming mixed-valence species (heteropolyblues and heteropolybrowns). Their characters, together with their solubility and stability in aqueous and non-aqueous solvents, make them suitable as photochromic,[6] electrochromic,[7] electrocatalytic and modified electrode[8] materials.

Practical applications of POM in these areas depend on the successful preparation of thin POM-containing films. Significant research efforts have been directed towards the entrapment of POM in polymeric networks,[9] into a sol–gel matrix[10] or their chemical anchoring to an organic backbone.[11] However, these coating techniques often result in a random orientation of POM sites in the film. To choose a rational immobilization method for improving the ordering and properties of such molecular assemblies, Clemente-Lenon *et al.*[12] prepared an ultrathin film containing heteropolyanion by using the Langmuir–Blodgett (LB) technique. However, with the LB technique it is difficult to construct larger size and thickness films.[13] Self-assembly is a very simple and powerful approach to construct supramolecular thin films on solid surfaces.[14] It has now been extensively explored in chemistry and material science as an effective strategy for fabricating a wide variety of complex ordered structures that are difficult or impossible to generate using traditional approaches.[15–17]

In the present work, we fabricate a layered nanocomposite film with a fine superlattice structure, and photochromic and electrochemical properties, from an ionic complex formed between a dimethyldioctadecylammonium (DODA) and a phosphomolybdate anion, $PMo_{12}O_{40}^{3-}$ (PMo_{12}) (the molecular structure is shown in Fig. 1), by supramolecular self-assembly.

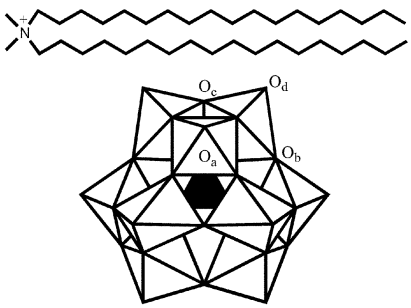

Fig. 1 (top) The DODA molecule. (bottom) The Keggin type polyanion $PMo_{12}O_{40}^{3-}$: O_a, oxygen atoms connected with MO_4 and XO_4 units; $O_{b,c}$, bridge oxygen atoms linking MO_4 octahedra from the same (O_c) or different (O_b) M_3O_{13}; O_d, external (corner) oxygen atoms.

Experimental

Materials

Phosphomolybdic acid ($H_3PMo_{12}O_{40}$) was prepared according to the literature method.[18] Dimethyldioctadecylammonium chloride was obtained from TCI (Japan). All other chemicals were of analytical grade and used as received. 0.24 mmol DODA was dispersed in 50 ml of water by sonication, to which was added 10 ml of aqueous $H_3PMo_{12}O_{40}$ (8 mM) with stirring. A yellow precipitate was collected by filtration, washed with water and dried. The composition of PMo_{12}–DODA was verified by elementary analysis. Found (%): C, 39.62; H, 7.08; N, 1.40; P, 0.85; Mo, 33.12. Calc. (%) for $3DODA^+ \cdot PMo_{12}O_{40}^{3-}$: C, 39.36; H, 6.96; N, 1.21; P, 0.89; Mo, 33.16. The molar ratio of DODA to $PMo_{12}O_{40}^{3-}$ was 3 : 1, consistent with the value expected from the electric charge balance between them. IR (cm^{-1}): 2950 (sh), 2919 (s), 2850 (s), 1482 (w), 1467 (m), 1062 (s), 955 (s), 880 (s), 797 (s), 721 (w).

Preparation of the self-assembled PMo_{12}–DODA film

Transparent thin films were obtained by casting a 0.1 mM chloroform solution of $3DODA^+ \cdot PMo_{12}O_{40}^{3-}$ on each of freshly cleaned hydrophilic borosilicate glass, CaF_2, and quartz substrates, for X-ray diffraction (XRD), Fourier transform infrared (FTIR), and UV–vis measurements. For cyclic voltammetry measurements, the working electrode was prepared by casting 3.0 μl of a chloroform solution of $3DODA^+ \cdot PMo_{12}O_{40}^{3-}$ (0.1 mM) on a glassy carbon electrode polished with 1.0, 0.3, and 0.05 μm α-Al_2O_3 powder successively and washed ultrasonically in pure water and ethanol. The electrode thus obtained was annealed at 70 °C and 5 °C in air before cyclic voltammetry measurement.

Measurement

C, H, and N elemental analyses were performed on a PerkinElmer 240C elemental analyzer; other elemental analyses were performed on a PerkinElmer 1000 ICP spectrometer. The XRD pattern in the low angle region was measured on borosilicate glass, with the diffraction vector perpendicular to the plane of the film using Cu Kα irradiation (λ = 1.5418 Å; angular resolution 0.02°) by a Rigaku D/max rA X-ray diffractometer. The phase transition temperatures of the composite film formed directly in the differential scanning calorimetry (DSC) sample pans were investigated by using a Mettler Toledo DSC 821^e instrument between 0 °C and 80 °C with a heating rate of 5 °C min^{-1}. The infrared and polarized infrared spectra were recorded with a Bruker IFS-66 spectrometer (Germany). The spectrum from 770 to 4000 cm^{-1} was obtained by using GE/KBr beam splitters, a globar lamp source, and a TGS detector. All absorption measurements were made on an UV–vis spectrophotometer (Shimadzu UV-1601PC) with 1 nm optical resolution over the range 190–1100 nm. The electron paramagnetic resonance (EPR) spectra of samples were recorded on a Bruker ER200-D-SRC spectrometer at X-band at 84 K. Photochromic experiments were carried out using a 500 W high-pressure mercury lamp as the light source. The distance between the lamp and the sample was 15 cm. Samples were maintained in contact with air during irradiation.

Electrochemical experiments were performed with a CHI 600 voltammetric analyzer (CH Instruments, USA) in a conventional three-electrode cell with a glassy carbon electrode or a glassy carbon electrode coated with a PMo_{12}–DODA film as the working electrode, a twisted platinum wire as the counter-electrode, and a Ag/AgCl (in saturated KCl solution) as the reference electrode, against which all potentials were measured and are reported in this article.

Results and discussion

IR spectra and polarized IR spectra

The arrangements of hydrocarbon chains in the nanocomposite film can be examined by IR spectra. In general, the vibration bands due to methylene asymmetrical stretching modes $\nu_{as}(CH_2)$ at 2915–2920 cm^{-1}, and methylene symmetrical stretching modes $\nu_s(CH_2)$ at 2846–2850 cm^{-1}, respectively, are indicative of the crystalline, highly ordered state of the hydrocarbon chains aggregates.[19] Fig. 2b shows the IR spectrum of the PMo_{12}–DODA composite film. The $\nu_{as}(CH_2)$ and $\nu_s(CH_2)$ appeared at 2918 and 2850 cm^{-1}, respectively. Thus, the arrangement of hydrocarbon chains in the composite film is highly ordered or crystalline. Note that besides the bands at 2918, 2850, and 1467 cm^{-1} assigned to the stretching vibrations and asymmetrical and symmetrical bending vibrations modes of CH_2 and CH_3 groups of the DODA alkyl chains, the IR spectrum of the PMo_{12}–DODA film shows very strong bands below 1200 cm^{-1}, due to the $PMo_{12}O_{40}^{3-}$. The bands in the composite film associated with the anions are narrower and generally slightly shifted when compared to the spectrum of the pure $H_3PMo_{12}O_{40}$ in a KBr pellet (Fig. 2a). They demonstrate that the $PMo_{12}O_{40}^{3-}$ polyanions are "trapped" in the composite film and their chemical structure is preserved. The narrower of the bands may be due to the different organization of the $PMo_{12}O_{40}^{3-}$ in the composite film or to the lower degree of hydration of the $PMo_{12}O_{40}^{3-}$ in the multilayers, compared to the crystalline state.[12b] Indeed, the strong bands around 3300–3500 and 1600–1650 cm^{-1} assigned to the stretching and bending modes of water are absent in the composite film. This demonstrates that the anions are largely dehydrated within the multilayers. A more detailed inspection of the vibration band shifts reveals that the Mo–O_d and P–O_a bands in the composite film have red shifts and the bands of Mo–O_b–Mo and Mo–O_c–Mo have blue shifts (Table 1). The shift observed for the different peaks is probably related to the organization and especially to the presence of positively charged DODA in the film.[12a] Indeed, Lavrencic-Stanger

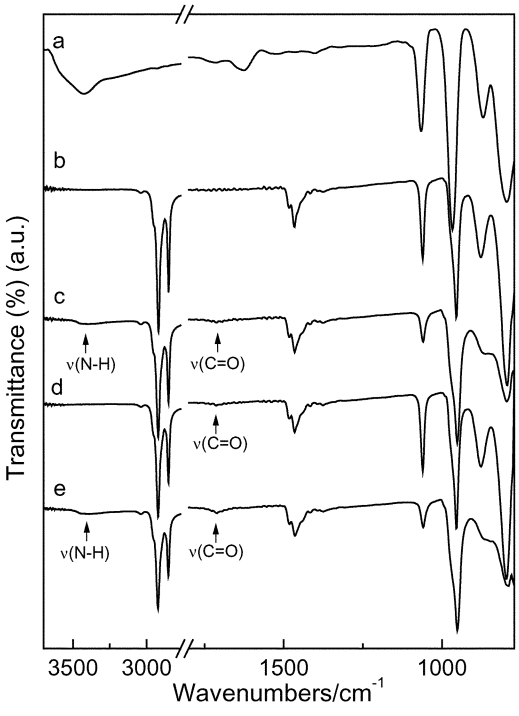

Fig. 2 FTIR spectra of: (a) $H_3PMo_{12}O_{40}$ polyanion in KBr pellet, (b) the PMo_{12}–DODA composite film without UV irradiation, (c) the composite film with UV irradiation for 80 min, (d) the coloration film after heating at 70 °C for 24 h, and (e) the second irradiation for 80 min after the PMo_{12}–DODA composite film has been bleached.

Table 1 Frequency values (cm^{-1}) and assignment of FTIR bands observed for the acid $H_3PMo_{12}O_{40}$, and the PMo_{12}–DODA[a] composite film

Assignment	$H_3PMo_{12}O_{40}$	PMo_{12}–DODA[b]	PMo_{12}–DODA[c]	PMo_{12}–DODA[d]
ν_1 Mo–O_b–Mo	793 (760–800)	795	791	795
ν_2 Mo–O_c–Mo	869 (840–910)	877	870	876
ν_3 Mo–O_d	963 (960–1000)	954	951	954
ν_4 P–O_a	1065 (1060–1080)	1060	1059	1060

[a]Values in parentheses indicate the range of frequencies found in the literature. [b]Without UV irradiation. [c]With UV irradiation for 80 min. [d]Coloration film after heating at 70 °C for 24 h.

et al.[20] observed similar shifts in the vibrations of $SiW_{12}O_{40}^{4-}$ and $PW_{12}O_{40}^{3-}$ incorporated into the 3-isocyanatopropyltriethoxysilane–poly(propylene glycol)bis(2-aminopropyl ether) (ICS-PPG) induced by the coulombic interactions between the heteropolyanions and the protonated polymeric supports. Peng and Wang[21] also found that a similar shift of the Keggin infrared bands in organic–inorganic salts formed by heteropolyoxometalates and other electron donors was induced by the coulombic interactions.

Another remarkable feature of the IR spectrum of the PMo_{12}–DODA composite film is the strong out-of-plane dichroism (Fig. 3). When the IR electrical field is not parallel to the plane of the substrate, new peaks corresponding to the $PMo_{12}O_{40}^{3-}$ can clearly be seen. This result shows that $PMo_{12}O_{40}^{3-}$ polyanions have one particular orientation (and distortion) in the multilayers, and that they can be oriented by the self-assembly technique.

Phase transition

Gel-to-liquid crystal phase transition is one of the fundamental properties of the bilayer membranes and is closely related to their thermal stability and structural regularity.[22] The phase transition peak of the PMo_{12}–DODA film was located at 45.6 °C with a ΔH value of 98.1 kJ mol^{-1}. This large ΔH value is indicative of the highly ordered packing of the amphiphilic component in the composite film. On the other hand, a PMo_{12}–tetrabutylammonium film obtained by casting *N*,*N*-dimethylformamide solution did not show any endothermic peak between 0 °C and 90 °C. This clearly indicates that the self-assembled PMo_{12}–DODA film possesses the typical thermal characteristic of the bilayer system.

X-ray diffraction

The periodicity of the bilayer structure in the film was investigated by XRD measurements. The composite film has more distinct (001), (002), and (003) Bragg peaks at 3.00°, 6.00°, and 9.04°, respectively, corresponding to *d* values of

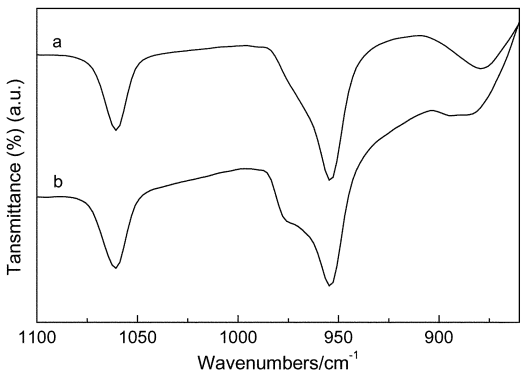

Fig. 3 Polarized infrared spectra of the PMo_{12}–DODA film. The angle between the plane of the substrate and the electric field is either 0° (a) or 45° (b).

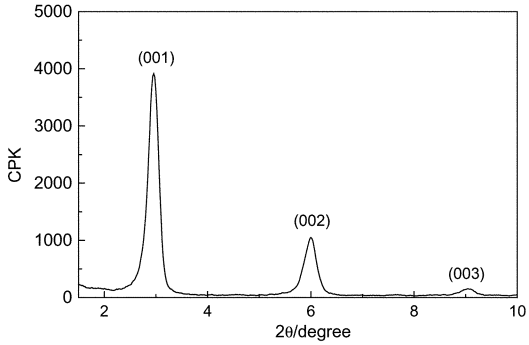

Fig. 4 XRD pattern of the self-assembled PMo_{12}–DODA composite film in the low angle region.

29.45, 14.73, and 9.78 Å (Fig. 4). These Bragg peaks indicate that the composite film forms a well-organized multi-bilayer structure with an interlayer spacing of 29.45 Å, which was smaller than that of the original DODA film (31 Å),[23] and suggests that the bilayer components become even more tilted. Considering the XRD result, the length of DODA (*ca.* 26.0 Å),[24] the radius of $PMo_{12}O_{40}^{3-}$ (*ca.* 5.2 Å), and the cross-sectional areas of $PMo_{12}O_{40}^{3-}$ (85 $Å^2$), calculated by its radius, and DODA (54 $Å^2$)[12a] (the cross-sectional area of two $PMo_{12}O_{40}^{3-}$ almost fits with that of three DODA molecules), a possible layered structure, to satisfy the geometric conditions and charge neutralization, is that two $PMo_{12}O_{40}^{3-}$ cluster ions are sandwiched between six monocationic DODA molecules, three in the lower layer and the other three in the upper layer (Fig. 5). This bilayer mode is very similar to that of Keggin polyanions in LB films, only the long spacing of the multi-bilayer film (29.45 Å) was about 60% of that for the LB film (49 Å),[12a] though both films were composed of the same DODA amphiphiles. This is in accordance with the well-known fact that the constituent amphiphilic molecules are less orientated in multi-bilayer films than in LB films.[23]

Photochromic behavior of the composite film

Typical absorption spectra of the PMo_{12}–DODA composite film before and after UV irradiation are shown in Fig. 6. Before UV irradiation there are only two strong characteristic absorption bands of $PMo_{12}O_{40}^{3-}$ at 222 nm and 314 nm, which are ascribed to the O_d–Mo and $O_{b,c}$–Mo charge-transfer transition bands, respectively. Both bands have a red shift compared to those of aqueous $H_3PMo_{12}O_{40}$ at 215 nm and 235 nm. We propose that the red shift may be attributed to compact arrays and identical orientation of the organic molecules, which made the big π-conjugated bonds of $PMo_{12}O_{40}^{3-}$ overlap partly. This overlap results in a decrease

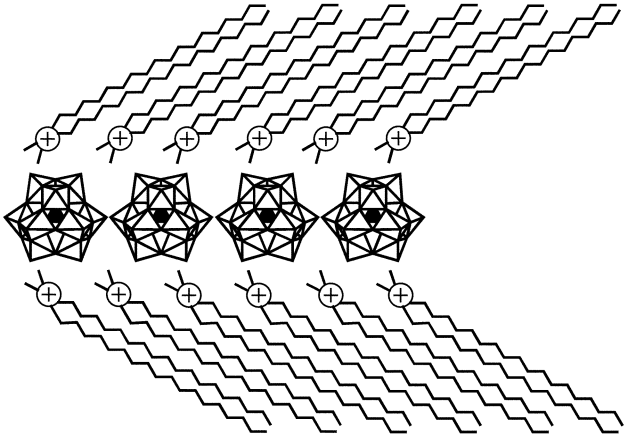

Fig. 5 The proposed model of the PMo_{12}–DODA composite film.

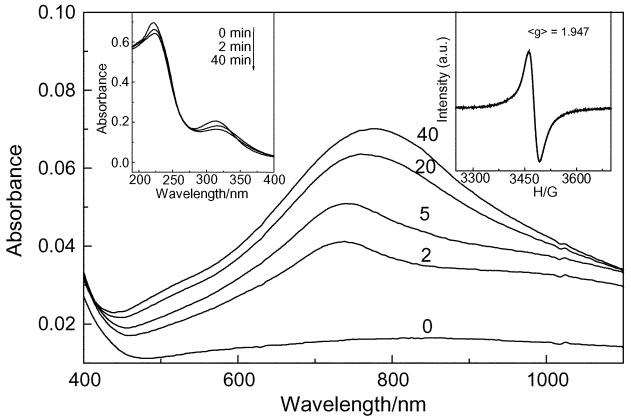

Fig. 6 Spectral changes at 400–1100 nm upon UV irradiation of the PMo_{12}–DODA composite film. Times (min) are indicated on the curves. Insets: Spectral changes at 190–400 nm and EPR spectrum of the composite film (irradiation time 40 min) at 84 K.

of intermolecular transition energy, thus the absorption bands have a red shift. After UV irradiation, a new broad absorption band having a maximum at about 770 nm, a shoulder at about 520 nm, and a weakening of the absorption peaks in the UV region are clearly observed; meanwhile, the film was colored with blue. Those bands are characteristic of reduced Keggin molecular species with d–d bands at about 555 nm and intervalence charge transfer (IVCT, $Mo^{5+} \rightarrow Mo^{6+}$) bands at about 769–625 nm.[5] The appearance of IVCT bands and the weakening of the absorption peaks in the UV region show that electron transfer occurs between the organic substrates and the heteropolyanions, converting the heteropolyanions to heteropolyblues with simultaneous oxidation of the organic substrates.

After the UV light was turned off, the films began to decolor gradually at room temperature in the dark. The decoloration is very slow so that it is not completed after 30 days. The bleaching could be promoted by heating at about 70 °C in air but not by visible light. By this means, the decoration could be completed in 1 day. The dependence of the change in absorbance on the bleaching time for the composite film at room temperature and 70 °C is shown in Fig. 7. If the UV irradiated films were stored in nitrogen, helium, argon or under vacuum conditions, it could retain the blue coloration for a long time. But on changing the ambient atmosphere back to air or oxygen, the bleaching process started again. These results show that oxygen plays an important role during the bleaching process.

Photochromic mechanism of the composite film

To explain the photochromic behavior of the film, it is necessary to investigate the variation of electronic structure of

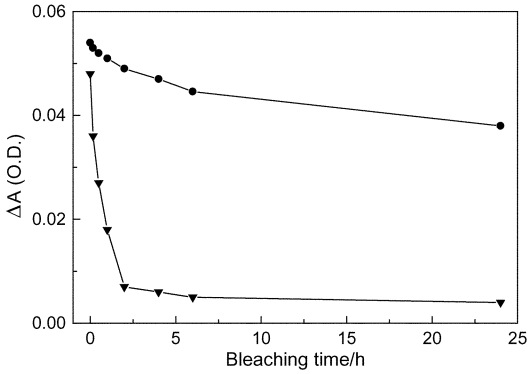

Fig. 7 The change of absorbance at 770 nm for the PMo_{12}–DODA film at room temperature (●) and at 70 °C (▼) as a function of the bleaching time.

the component in the composite film during the photochromic process so as to make clear the photochromic mechanism. EPR analysis is an efficient and sensitive way of characterizing POM. The unirradiated samples exhibit no significant EPR signals at 84 K. But after UV irradiation the composite film showed a significant defined signal, which is shown in the inset of Fig. 6. The signal is ascribed to Mo^{5+} with $g = 1.937$, which is in agreement with values reported in the literature.[25] Observation of a UV-induced EPR signal suggests electron transfer in the lattice and that $PMo_{12}O_{40}^{3-}$, acting as an acceptor, obtains electrons during UV irradiation.

The changes of IR spectra for the composite film after UV irradiation are another powerful indication that DODA is oxidized and $PMo_{12}O_{40}^{3-}$ reduced in the photochromic process. As shown in Fig. 2c and Fig. 2e, after UV irradiation the intensity of the set of bands relating to $PMo_{12}O_{40}^{3-}$ is decreasing strongly, meanwhile, a slight shift (Table 1) and a broadening of these bands are detectable, which results from the formation of heteropolyblue.[26] It indicates that the $PMo_{12}O_{40}^{3-}$ polyanions obtain electrons and are reduced. Simultaneously, two new bands around 1710 cm^{-1} and 3350 cm^{-1} appear, corresponding to the formation of carbonyl bonds (C=O) and nitrogen hydrogen bonds (N–H) of secondary amine due to oxidation of DODA. Moreover, the intensity of the vibrations corresponding to these two groups increases with prolonged irradiation time, which indicates that the content of C=O and N–H increases with increasing irradiation time. After decoloration at 70 °C in air, the frequencies of all characteristic vibrational bands of $PMo_{12}O_{40}^{3-}$ are restored (Fig. 2d and Table 1).

We suppose that the photochromic mechanism of the composite film is electron transfer from the positively charged $[(CH_3)_2N(C_{18}H_{37})_2]^+$ to the negatively charged $[PMo_{12}O_{40}]^{3-}$, which is similar to the photochromic mechanism of $[NBu_4]_4[W_{10}O_{32}]$ in acetonitrile proposed by Yamase *et al.*[27] The photochromic mechanism of the composite film can be denoted as the following equations.

$$\text{Coloration: } [(CH_3)_2N(C_{18}H_{37})_2]^+ + [PMo_{12}O_{40}]^{3-} + h\nu \rightarrow [(CH_3)_2N(C_{18}H_{37})^{\bullet}]^+ + [PMo_{12}O_{40}]^{4-} + H^+ + \text{1-octadecylene} \quad (1)$$

$$\text{Decoloration: } [PMo_{12}O_{40}]^{4-} + O_2 \rightarrow [PMo_{12}O_{40}]^{3-} \quad (2)$$

In eqn. (1), the radical cation $[(CH_3)_2N(C_{18}H_{37}^{\bullet})]^+$ may undergo deprotonation, disproportionation, and hydrolysis in the presence of water (in this case it means the water in air) to yield octadecylaldehyde, dimethyloctadecylamine and dimethylamine ($[(CH_3)_2N(C_{18}H_{37})^{\bullet}]^+ - H^+ \rightarrow (CH_3)_2\dot{N}CH–C_{17}H_{35} \rightarrow 1/2(CH_3)_2N–C_{18}H_{37} + 1/2(CH_3)_2NCH{=}CH–C_{16}H_{33}$, $(CH_3)_2NCH{=}C(\dot{C})H–C_{16}H_{33} + H_2O \rightarrow (CH_3)_2NH + C_{17}H_{35}CHO$. For the decoloration process [eqn. (2)], O_2 can oxidize Mo^{5+} into Mo^{6+}.

Electrochemical behavior of the composite film

To investigate the influence of DODA cations in the composite film on the electrochemical properties of $PMo_{12}O_{40}^{3-}$, the electrochemical behavior of $PMo_{12}O_{40}^{3-}$ in aqueous solution was first studied. The cyclic voltammograms of $PMo_{12}O_{40}^{3-}$ in homogeneous solution shows three, reversible, two-electron waves in the potential range between −0.2 and +0.6 V (Fig. 8b). As shown in Fig. 8a, the cyclic voltammograms of the PMo_{12}–DODA composite film also present three reversible well-defined redox couples with mean peak potentials of −0.10, +0.14, and +0.27 V and a peak to peak separation of less than 30 mV. Compared with curve b, the formal potentials shift slightly negative, which may be related to the presence of long-chain lipids.[28] From curve a and b, we can see that the

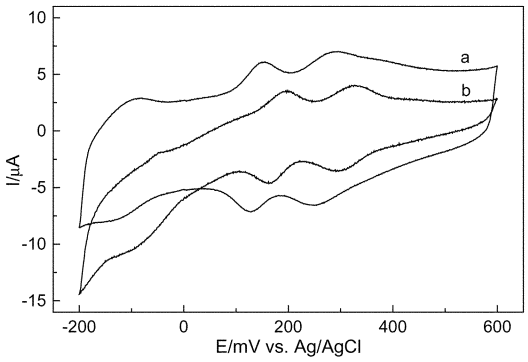

Fig. 8 Cyclic voltammograms of a naked glassy carbon electrode in 1 mM $H_3PMo_{12}O_{40}$ solution of pH 1.0 (a) and a glassy carbon electrode coated with PMo_{12}–DODA film (b) in an H_2SO_4 aqueous solution of pH 1.0 with a scan rate of 50 mV s^{-1}.

electrochemical behavior of the PMo_{12}–DODA composite film is similar to that of $PMo_{12}O_{40}^{3-}$ in homogeneous solution.

Fig. 9 shows cyclic voltammograms of the composite film electrode at different scan rates in the potential range +0.6 to −0.2 V in pH 1.0 H_2SO_4 solution. The peak currents increased linearly with the scan rates between 10 and 200 mV s^{-1} (inset in Fig. 9), as expected for a surface process. We consider that the electrochemical reaction of $PMo_{12}O_{40}^{3-}$ in the composite film is facile and can also be easily oxidized and reduced.

In general, the reduction of heteropolyanions is accompanied by protonation, therefore, the pH of the solution has a great effect on the electrochemical behavior of the heteropolyanions. As we know, $PMo_{12}O_{40}^{3-}$ anions are stable in aqueous media at pH < 4.0. Beyond this pH range, $PMo_{12}O_{40}^{3-}$ anions become unstable due to hydrolytic decomposition.

Fig. 10 shows the dependence of the anodic peak potentials (E_{pa}) of the PMo_{12}–DODA composite film on a modified glassy carbon electrode on the pH of the solution. In a pH of less than 4.0, as pH increases, the shapes of the redox peaks remain unchanged, the peak potentials shift negatively. Plots of E_{pa} *versus* pH for the composite film have a linear region from 0.5 up to 4.0. The average slopes of the three redox couples in this pH range are −58, −63, and −63 mV pH^{-1}, respectively, which are close to the theoretical value of −60 mV pH^{-1} for $2e^-/2H^+$. It is confirmed that, in the composite film, the two-electron process is accompanied by a two-protonation reaction.

The above results allow us to describe the three overall redox processes of the PMo_{12}–DODA composite film on a modified

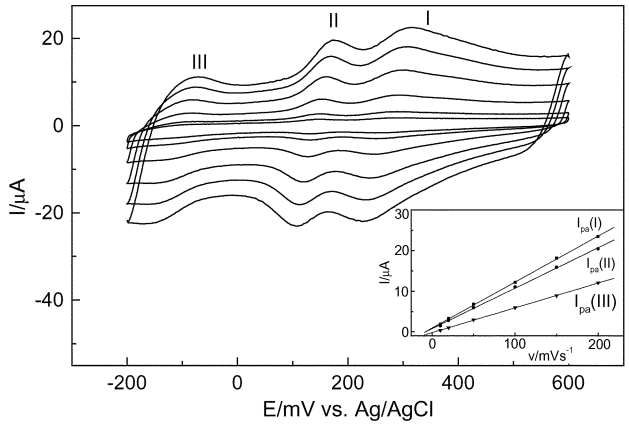

Fig. 9 Cyclic voltammograms of a PMo_{12}–DODA composite film modified glassy carbon electrode in pH 1.0 H_2SO_4 at different scan rates (from inner curve to outer curve: 10, 20, 50, 100, 150, 200 mV s^{-1}). The inset shows variation of peak current I_{pa} with scan rates.

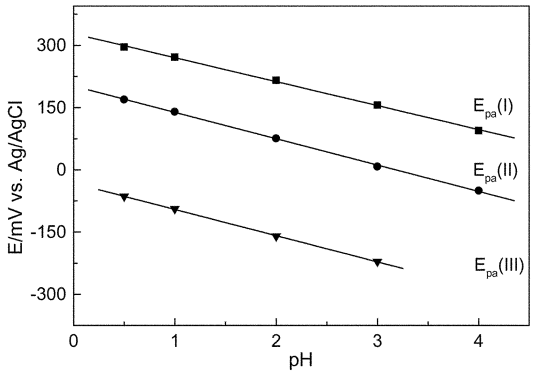

Fig. 10 Dependence of the anodic peak potentials on the pH values of the solution.

glassy carbon electrode in acidic solution of pH less than 4.0 as follows:

$$PMo_{12}O_{40}^{3-} + 2e^- + 2H^+ \rightleftharpoons H_2PMo_2^{V}Mo_{10}^{VI}O_{40}^{3-}$$

$$H_2PMo_2^{V}Mo_{10}^{VI}O_{40}^{3-} + 2e^- + 2H^+ \rightleftharpoons H_4PMo_4^{V}Mo_8^{VI}O_{40}^{3-}$$

$$H_4PMo_4^{V}Mo_8^{VI}O_{40}^{3-} + 2e^- + 2H^+ \rightleftharpoons H_6PMo_6^{V}Mo_6^{VI}O_{40}^{3-}$$

The same redox process of the PMo_{12}–DODA composite film as that of $PMo_{12}O_{40}^{3-}$ in solution may suggest that protonation–deprotonation is almost unhindered by the electrostatic interaction between DODA and $PMo_{12}O_{40}^{3-}$. The composite film can provide a favorable environment for electron and proton transference.

The stability of the modified electrode was tested by measuring the decrease in voltammetric currents during potential cycling of the modified electrode. The composite film electrode containing $PMo_{12}O_{40}^{3-}$ showed a high stability. For example, when in the potential range from −0.2 to +0.6 V (*vs.* SCE) and in pH 1.0 solution, the composite film was subjected to 30 potential cycles, no decrease in the steady-state voltammetric currents was observed. When the PMo_{12}–DODA composite film was placed in air for several days, the current response remained almost unchanged in the film.

The dependence of cyclic voltammograms of the composite film on the irradiation of UV light is shown in Fig. 11. With a prolonged irradiation time, the redox potentials shift slightly negative and the redox peak current decreased gradually, which suggested that intermolecular charge-transfer occurred and Mo^{6+} was photoreduced to Mo^{5+} under UV irradiation.[29] This is further proof that coloration of the film results from electron transfer between $PMo_{12}O_{40}^{3-}$ and DODA.

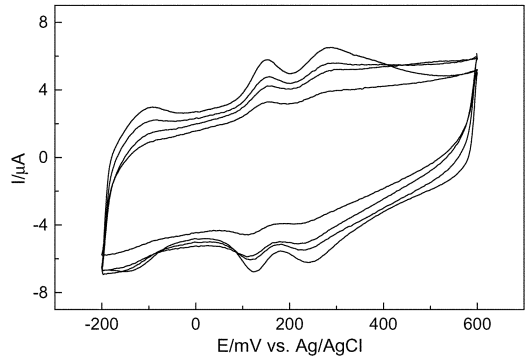

Fig. 11 Dependence of cyclic voltammograms of the composite film on the UV light irradiation (from inner curve to outer curve: 40, 20, 10, 0 min).

Conclusions

A layered superlattice self-assembled multilayer film has been fabricated. The IR spectra showed that the Keggin structure of $PMo_{12}O_{40}^{3-}$ is preserved in the composite film. From XRD, DSC, the length of the DODA, the radius of $PMo_{12}O_{40}^{3-}$, and the cross-sectional area of them, a possible structural model was proposed. Each inorganic layer consists of one PMo_{12} monolayer incorporated into a hydrophilic interlayer with an interlayer spacing of 29.45 Å. $PMo_{12}O_{40}^{3-}$ incorporated in the bilayer film keeps its inherent photochemical and electrochemical properties intact. When exposed to UV light, the films turn blue due to the reduction of $PMo_{12}O_{40}^{3-}$ and oxidation of DODA. Bleaching can occur when the material is in contact with ambient air or O_2, which can be promoted by heating in air. According to the experimental results, we proposed that the photochromic mechanism of the composite film was according to a radical process. The electrochemical behavior of the modified electrodes with the self-assembled PMo_{12}–DODA composite film were investigated by cyclic voltammetry in acidic aqueous solutions. The modified electrode showed many advantages, such as simple fabrication, good chemical and mechanical stability and independence of electrode size and topology. The facile electrochemistry of the composite film will probably be used to prepare a sensitive conductometric catalytic electrode and to construct thin film molecular electronic devices based on heteropolyanions in future work. The preliminary results indicate that new lamellar organized materials with photochromic, electrochromic, and electrochemical properties can be fabricated *via* self-assembly. In fact, the appropriate choice of POM and lipid molecule should be helpful for fabricating functional ordered films having optical, magnetic, catalytic, electrocatalytic, electrochromic and photochromic properties.

Acknowledgement

The authors acknowledge the National Natural Science Foundation of China (NNSFC) for the provision of financial support.

References

1 V. Kozhevnikov, *Chem. Rev.*, 1998, **98**, 171.
2 F. Busserean, M. Piacard, C. Malik, A. Teze and J. Blancen, *Ann. Inst. Pasteur/Virol.*, 1988, **32**, 33.
3 K. Ono, H. Nakane, F. Barre-Sinoussi and C. Chermann, *Nucleic Acids Res. Symp. Ser.*, 1984, **15**, 169.
4 (*a*) M. T. Pope and A. Muller, *Angew. Chem., Int. Ed. Engl.*, 1991, **30**, 34; (*b*) D. E. Katsoulis, *Chem. Rev.*, 1998, **98**, 359.
5 M. T. Pope, *Heteropoly and Isopoly Oxometalates*, Springer-Verlag, Heidelberg, 1983.
6 (*a*) T. Yamase, *Chem. Rev.*, 1998, **98**, 307; (*b*) P. Gomez-Romero and N. Casan-Pastor, *J. Phys. Chem.*, 1996, **100**, 12448.
7 (*a*) X. M. Zhang, B. Z. Shan, Z. P. Bai, X. Z. You and C. Y. Duan, *Chem. Mater.*, 1997, **9**, 2687; (*b*) I. Moriguchi and J. H. Fendler, *Chem. Mater.*, 1998, **10**, 2205.
8 (*a*) L. Cheng, L. Niu, J. Gong and S. J. Dong, *Chem. Mater.*, 1999, **11**, 1465; (*b*) D. Ingersoll, P. J. Kulesza and L. R. Faulker, *J. Electrochem. Soc.*, 1994, **14**, 140; (*c*) B. Keita, K. Essaadi and L. Nadjo, *J. Electroanal. Chem.*, 1989, **259**, 127; (*d*) A. Kuhn and F. C. Anso, *Langmuir*, 1996, **12**, 5481.
9 (*a*) M. Lira-Cantu and P. Gomez-Romero, *Chem. Mater.*, 1998, **10**, 698; (*b*) P. Gomez-Romero and M. Lira-Cantu, *Adv. Mater.*, 1997, **9**, 144; (*c*) M. Clemente-Leon, E. Coronado, J. R. Galan-Mascaros, C. Gimenez-Saiz, C. J. Gomez-Garcia and T. Fernandeza-Otero, *J. Mater. Chem.*, 1998, **8**, 309.
10 (*a*) T. R. Zhang, W. Feng, C. Y. Bao, R. Lu, X. T. Zhang, T. J. Li, Y. Y. Zhao and J. N. Yao, *J. Mater. Res.*, 2001, **16**, 2256; (*b*) P. Judeinstein, P. W. Oliveria, H. Krug and H. Schmidt, *Chem. Phys. Lett.*, 1994, **220**, 35; (*c*) Y. G. Mo, R. O. Dillon, P. G. Snuder and T. E. Tiwald, *Thin Solid Films*, 1999, **335**(336), 1.
11 (*a*) P. Judeinstein, *Chem. Mater.*, 1992, **4**, 4; (*b*) C. R. Mayer, R. Thouvenot and T. Lalot, *Macromolecules*, 2000, **33**, 4433.
12 (*a*) M. Clemente-Leon, B. Agricole, C. Mingotaud, C. J. Gomez-Garcia, E. Coronado and P. Delhaes, *Langmuir*, 1997, **13**, 2340; (*b*) M. Clemente-Leon, B. Agricole, C. Mingotaud, C. J. Gomez-Garcia, E. Coronado and P. Delhaes, *Angew. Chem., Int. Ed. Engl.*, 1997, **36**, 1114.
13 (*a*) Y. J. Zhang, L. S. Li, J. Jin, S. M. Jiang, Y. Y. Zhao, T. J. Li, X. G. Du and S. Q. Yang, *Langmuir*, 1999, **15**, 2183; (*b*) J. Jin, L. S. Li, Y. J. Zhang, Y. Q. Tian, S. M. Jiang, Y. Y. Zhao, Y. B. Bai and T. J. Li, *Langmuir*, 1998, **14**, 5131.
14 (*a*) M. Lehn, *Science*, 1993, **260**, 1762; (*b*) G. M. Whitesides, J. P. Mathias and C. T. Seto, *Science*, 1991, **254**, 1312.
15 (*a*) Y. Lvov, K. Aviga, I. Ichinose and T. Kunitake, *J. Am. Chem. Soc.*, 1995, **117**, 6117; (*b*) I. Ichinose, T. Kawakami and T. Kunitake, *Adv. Mater.*, 1998, **10**, 535.
16 S. Y. Oh, Y. J. Yun, D. Y. Kim and S. H. Han, *Langmuir*, 1999, **15**, 4690.
17 (*a*) Z. H. Chen, Y. A. Yang, J. B. Qiu and J. N. Yao, *Langmuir*, 2000, **16**, 722; (*b*) M. Dreja, I. T. Kim, Y. D. Yin and Y. N. Xia, *J. Mater. Chem.*, 2000, **10**, 603; (*c*) K. Tsuda, G. C. Dol, T. Gensch, J. Hofkens, L. Latterini, J. W. Weener, E. W. Meijer and F. C. De-Schryver, *J. Am. Chem. Soc.*, 2000, **12**, 3445.
18 C. Rocchiccioli-Deltcheff, M. Fournier, R. Franck and R. Thouvenot, *Inorg. Chem.*, 1983, **22**, 207.
19 (*a*) H. H. Mantsch and R. N. Mcelhany, *Chem. Phys. Lipids*, 1991, **57**, 213; (*b*) N. E. Schlotler, M. D. Porter, T. G. Bright and D. L. Allara, *Chem. Phys. Lett.*, 1986, **132**, 93; (*c*) R. G. Snyder, *J. Mol. Spectrosc.*, 1960, **4**, 411.
20 U. Lavrencic-Stanger, N. Groselj, B. Orel and Ph. Colomban, *Chem. Mater.*, 2000, **12**, 745.
21 J. Peng and E. B. Wang, *J. Mol. Struct.*, 1998, **444**, 213.
22 N. Higashi, T. Kajiyama, T. Kunitake, W. Pass, H. Ringsdorf and A. Takahara, *Macromolecules*, 1987, **20**, 29.
23 I. Morriguchi, N. Fujiyoshi, R. Sakamoto, Y. Teraoka and S. Kagawa, *Colloids Surf. A*, 1997, **126**, 159.
24 J. F. Rusling and H. P. Zhang, *Langmuir*, 1991, **7**, 1791.
25 M. T. Pope, *Mixed-Valence Compounds, Heteropoly Blues*, Reidel, Oxford, 1979.
26 (*a*) E. B. Wang, L. Xu and R. D. Huang, *Sci. Sin., Ser. B*, 1991, **11**, 1121; (*b*) L. C. Hill and A. D. Bouchaod, *J. Am. Chem. Soc.*, 1985, **107**, 5148.
27 T. Yamase, N. Takabayashi and M. Kaji, *J. Chem. Soc., Dalton Trans.*, 1984, **5**, 793.
28 S. Liu, Z. Tang, E. Wang and S. Dong, *Thin Solid Films*, 1999, **339**, 277.
29 S. Z. Liu, Z. Wang and Z. J. Ku, *J. Hubei Univ. (Nat. Sci. Ed.)*, 1998, **20**, 260.